

SOSeas Web App: An assessment web-based decision support tool to predict dynamic risk of drowning on beaches using deep neural networks

Javier García-Alba, Javier F. Bárcena, Luis Pedraz, Felipe Fernández, Andrés García, Marcos Mecías, Javier Costas-Veigas, María Luisa Samano & David Szpilman

To cite this article: Javier García-Alba, Javier F. Bárcena, Luis Pedraz, Felipe Fernández, Andrés García, Marcos Mecías, Javier Costas-Veigas, María Luisa Samano & David Szpilman (2021): SOSeas Web App: An assessment web-based decision support tool to predict dynamic risk of drowning on beaches using deep neural networks, *Journal of Operational Oceanography*, DOI: [10.1080/1755876X.2021.1999107](https://doi.org/10.1080/1755876X.2021.1999107)

To link to this article: <https://doi.org/10.1080/1755876X.2021.1999107>



Published online: 08 Nov 2021.



Submit your article to this journal



View related articles



View Crossmark data

CrossMark



SOSeas Web App: An assessment web-based decision support tool to predict dynamic risk of drowning on beaches using deep neural networks

Javier García-Alba^a, Javier F. Bárcena^a, Luis Pedraz^a, Felipe Fernández^a, Andrés García^a, Marcos Mecías^{b,c}, Javier Costas-Veigas^b, María Luisa Samano^{b,c,d} and David Szpilman^{e,f,g,h,i}

^aIHCantabria - Instituto de Hidráulica Ambiental de la Universidad de Cantabria, Santander, Spain; ^bUniversidad Europea del Atlántico, Santander, Spain; ^cCentro de Investigación y Tecnología Industrial de Cantabria (CITICAN), Santander, Spain; ^dUniversidad Internacional Iberoamericana, Campeche, Mexico; ^eBrazilian Life Saving Society, Rio de Janeiro, Brazil; ^fRio de Janeiro Fire Department (CBMERJ), Brazil; ^gCivil Defense, Rio de Janeiro, Brazil; ^hInternational Lifesaving Federation, Brussels, Belgium; ⁱInternational Drowning Researchers' Alliance, Lisbon, Portugal

ABSTRACT

People still drown on beaches in unacceptable numbers due to the lack of knowledge about the risks taking place in them. The proposed methodology forecasts electronic bathing flags in beaches by integrating the benefits of metocean operational systems, machine learning and web-based decision support technologies into a 24/7 risk assessment service that could be easily implemented at any beach worldwide with low costs of maintenance. Firstly, a crosscutting analysis between metocean conditions, beach characteristics and flag records was performed. Secondly, an expert system, based on Deep Learning, was developed to obtain electronic bathing flags as an indicator of the dynamic risk of drowning on beaches. The input variables of the Deep Neural Network were significant wave height, mean wave period, wind velocity, marine current velocity, incidence angle, and beach modal state. Finally, the application of the method to the Santa Catarina's beaches (Brazil) conveniently reproduced the status flag of beaches.

ARTICLE HISTORY

Received 10 December 2020
Accepted 9 September 2021

Highlights

- DNN forecast electronic bathing flags using metocean conditions and beach characteristics.
- DNN are viable surrogates of highly nonlinear process-based models.
- Beach users and lifeguards use this system as a decision support tool.
- The tool provides information about future scenarios without real modelling.
- The tool has created the availability to enhance safety on beaches.

1. Introduction

The 17 UN Sustainable Development Goals (SDGs) were proposed at the United Nations Conference on Sustainable Development in Rio de Janeiro in 2012 to meet the urgent environmental, political, and economic challenges facing the world. Goal 3 of the SDGs focuses on 'ensuring healthy lives and promoting well-being at all ages'.

Around 372,000 people per year die by drown (WHO 2014). This is why drowning is one of the main causes of death worldwide and the third leading cause of unintentional injury death. Drowning is among the ten leading causes of death for children and young people in every region of the world (WHO 2014). Nevertheless, the registered data underestimates the real problem of public health related to drowning because the total number of deaths from drowning may be 50% more than recorded in developed countries (Lunetta et al. 2004) and could be five times higher in developing countries (Peden et al. 2008). For instance, the maximum drowning index in Latin America is located in Brazil, where a person dies by drowning every 91 min (Szpilman et al. 2012). Due to this high number of drownings, several Brazilian institutions have been collecting data since 2009 as reported by lifeguards (legally responsible for lifeguarding at Brazilian beaches). This data is a valuable information for quantifying the drowning risk at beaches and to setting up an assessment tool.

Despite significant advancements in technology, techniques and knowledge, people still drown on the

coast in unacceptable numbers due to the lack of knowledge about the possible risks that take place in aquatic systems. Thus, drowning and accidents in aquatic systems are an unresolved worldwide problem and considered as a public health issue. Consequently, there is an urgent need to tackle this issue to reduce the number of compromised human lives by increasing research, development and innovation in this field. Against this backdrop, the following question arises: could we develop a worldwide operational system to inform end-users about the risks at any patrolled or unpatrolled beach?

Usually, process-based models have been directly used to provide information for risk analysis (Gómez et al. 2014; Cid et al. 2014; Gómez et al. 2015; Cid et al. 2017; Chiri et al. 2019) or by means of hybrid downscaled systems in local areas of aquatic systems (Camus et al. 2011; 2017; Bárcena et al. 2016, 2017). Notwithstanding the increase in computer power, process-based model complexity is also growing at the same rate, if not faster (Washington et al. 2009), suggesting that computational requirements will be an impediment to applications where a quick answer is required, e.g. managing the temporary closures of bathing sites due to metocean conditions. Therefore, these approaches are not operative in generating a worldwide system capable of offering a risk forecast of drowning as a function of hydrodynamic information and beach characterisation.

Accordingly, different techniques have been proposed in the last few years to overcome the large computational burden associated with process-based models, called dynamic emulation modelling (Castelletti et al. 2012). An emulator is a computationally efficient low-order model identified from the original large model and then used to replace it for computationally intensive applications. In the field of hydrodynamic and water quality, data-based models such as Artificial Neural Networks (ANN) are efficient in analysing behaviour along the coast and, hence, serve as surrogates for computationally demanding process-based models (van der Merwe et al. 2007; Zeng et al. 2015; Chiri et al. 2019; García-Alba et al. 2019).

In recent years, ANNs are evolving into Deep Neural Networks (DNN), the most distinguishing characteristic of DNNs from non-deep neural networks or ANNs is the depth of the network, provided by the stacking of multiple neuron layers in combinatorial and carefully designed architectures (Shen 2018). The main advantages of DNN are: (1) Large-depth network structures provide the ability to model highly complex functions, spatiotemporal dependences, and data distributions from big data (Schmidhuber 2015); (2) it allows the

automatic extraction and engineering of a cascade of abstract features from raw data (Bengio et al. 2013); (3) after knowledge on how to extract these features is learned and stored in the form of trained network weights, these networks can enable transfer learning (reuse of the model trained on one task to another task), greatly extending the value of available training data (Yosinski et al. 2014); (4) increased network depth allows exponential growth of the ability to represent complex functions (Raghu et al. 2016).

Although DNN models need to be trained and validated, which is a time-consuming process, one of the most valuable characteristics of DNNs is their ability to perform long-term forecasting with computational times that barely exceed one minute. Furthermore, the longer the forecasting period, the greater the reduction in computational time by DNN models. From a technical perspective, DNN models have a strong predictive ability for nonlinear systems enabling it to be synchronised with another system and can enhance the overall reliability and applicability of process-based models simplifying the mathematical descriptions of the physical structure and mechanism of chaotic systems (Goh et al. 2017). From the operational perspective, the implementation of DNN models is highly efficient at a very low computational cost compared to the implementation of process-based models (García-Alba et al. 2019). This capability is particularly useful in scenarios where on-the-spot decisions are needed (e.g. temporary closure of beaches), for which the use of complex and detailed process-based models can be cumbersome.

Additionally, the daily environmental information produced by the Copernicus Programme holds huge potential for the creation of real-time insights for decision-making support. The Copernicus Marine Environment Monitoring Service (CMEMS) provides regular and systematic reference information on the physical state and dynamics of the ocean and marine ecosystems for the global ocean and the European regional seas (Traon et al. 2019). Using this information, together with other relevant metocean data products provided by the Copernicus Climate Service (C3S) and the U.S National Oceanic and Atmospheric Administration (NOAA), we propose a downstream service to reduce the third leading cause of unintentional injury leading to death worldwide.

Therefore, this study aims to reduce drowning and accidents in aquatic spaces through the development of an assessment tool for predicting the dynamic risk of drowning on beaches categorised by electronic bathing flags, namely the SOSeas Service. In order to achieve the successful development of the SOSeas Service, the following specific objectives were stated: (1) Obtain

the cross-reference analysis between historic metocean conditions and the catalogue of events; (2) Setup a DNN that allows the identification of risks derived from dynamic metocean conditions; (3) Development of an operational system that integrates the DNN and the metocean conditions (real time and forecasting) to provide tailored information about the dynamic and static risks of the beach as displayed with electronic bathing flags.

The developed assessment tool has been implemented in Brazilian beaches with different characteristics and enough information of incidents to feed a computer tool with a core based on DNNs according to the information provided by the Brazilian Life Saving Society (SOBRASA) and metocean data available under open access. Section 2 provides a brief description of Santa Catarina's beaches (henceforth SCB), located in Brazil and selected as the study area for this work. In Section 3, we describe DNN and present the proposed methodology. The application of the methodology to the SCB is described in detail in Section 4. Finally, the discussion and conclusions of this work are provided in Section 5 and Section 6, respectively.

2. Study area and available data

The SOSeas Web App has been prototyped and implemented in the Santa Catarina's beaches (SCB), located in southern Brazil between 26° and 29.3°S, where firefighters are in charge of lifeguarding activities ([Figure 1](#)). The coast contains 922 km of open coast and bay shoreline with 246 sandy beaches, occupying 60% of the shore ([Oliveira et al. 2014](#)). It runs south and then southwest for about 430 km.

Tides are small, with deep-water waves averaging 1.5 m arriving from the east through south ([Pianca et al. 2010](#)). Most of the open coast faces east to southeast and is composed of fine to medium sand resulting in predominately wave-dominated beaches, with tide-modified and tide-dominated beaches occurring in a few very sheltered embayments and within the larger North and South bays ([A. H. da Klein et al. 2016](#)).

Consequently, SCBs have numerous hazardous beaches characterised by variable surf zone morphology (bars, channels and troughs) or variable surf zone currents (onshore, longshore and offshore); including strong narrow rip currents, together with breaking waves. Furthermore, the abundance of coastal environments combined with a mild subtropical climate has resulted in the use of the coast traditionally for fishing and transport, and more recently for housing, recreation, bathing, surfing, and general tourism ([Polette and Raucci 2003](#)).

All of these factors present a physical hazard to beach users. The result of the interaction of beach users with these hazards has been a level of risk involving accidents leading to rescues and first aid, and in some cases, drowning. To mitigate this risk, lifeguards patrol most of the popular beaches particularly during the summer vacation periods. However, even with lifeguards, rescues and drowning are at an unacceptably high rate, in common with much of the Brazilian coast ([Szpilman et al. 2012](#)).

SOBRASA manages the SCB flag warnings data catalogue, which provided information on 346 lifeguard posts from 139 coastal beaches (see [Figure 1](#)) from November 2016 to July 2019, including local environmental observations from lifeguards. [Table 1](#) provides more information about the beach flag warnings data catalogue with 79,487 records. The meaning of the warning flags used along the SCB are: (1) Green flags indicate low hazard with calm conditions (exercise caution); (2) Yellow flags indicate medium hazard from moderate surf and/or currents; (3) Red flags indicate high hazard from high surf and/or strong currents.

The DNN development requires, on the one hand, the geomorphological characteristics of beaches, such as their beach orientation or modal state (see [Figure 1](#)). This data was obtained from the work by Klein et al. ([2016](#)) and Quetzalcóatl et al. ([2019](#)). On the other hand, the DNN development requires metocean variables coming from reanalysis products that provide past metocean conditions worldwide. [Table 2](#) lists the reanalysis providers, products, and variables used in the SOSeas Web Service.

Once the DNN has been set up, metocean forecasting products can be used to forecast the electronic beach flag. [Table 2](#) shows the forecasting providers, products, and variables implemented in the SOSeas Service. Although the service has been implemented in Brazil, it has been designed to be implemented globally; therefore, global and open metocean products from reanalysis and forecasting are used.

3. Methods and material

3.1. Deep neural networks

The basic structure of DNNs is characterised by their architecture, activation functions, and training algorithm. The DNN architecture consists of three types of layers (see [Figure 2](#)): one input layer, n hidden layers, and one output layer ([Khalil et al. 2011](#)). Every layer has several nodes that are responsible for transmitting the information from one layer to the next layer, although neither lateral connection within any layer nor feedback connection is possible (arrows in [Figure 2](#)).

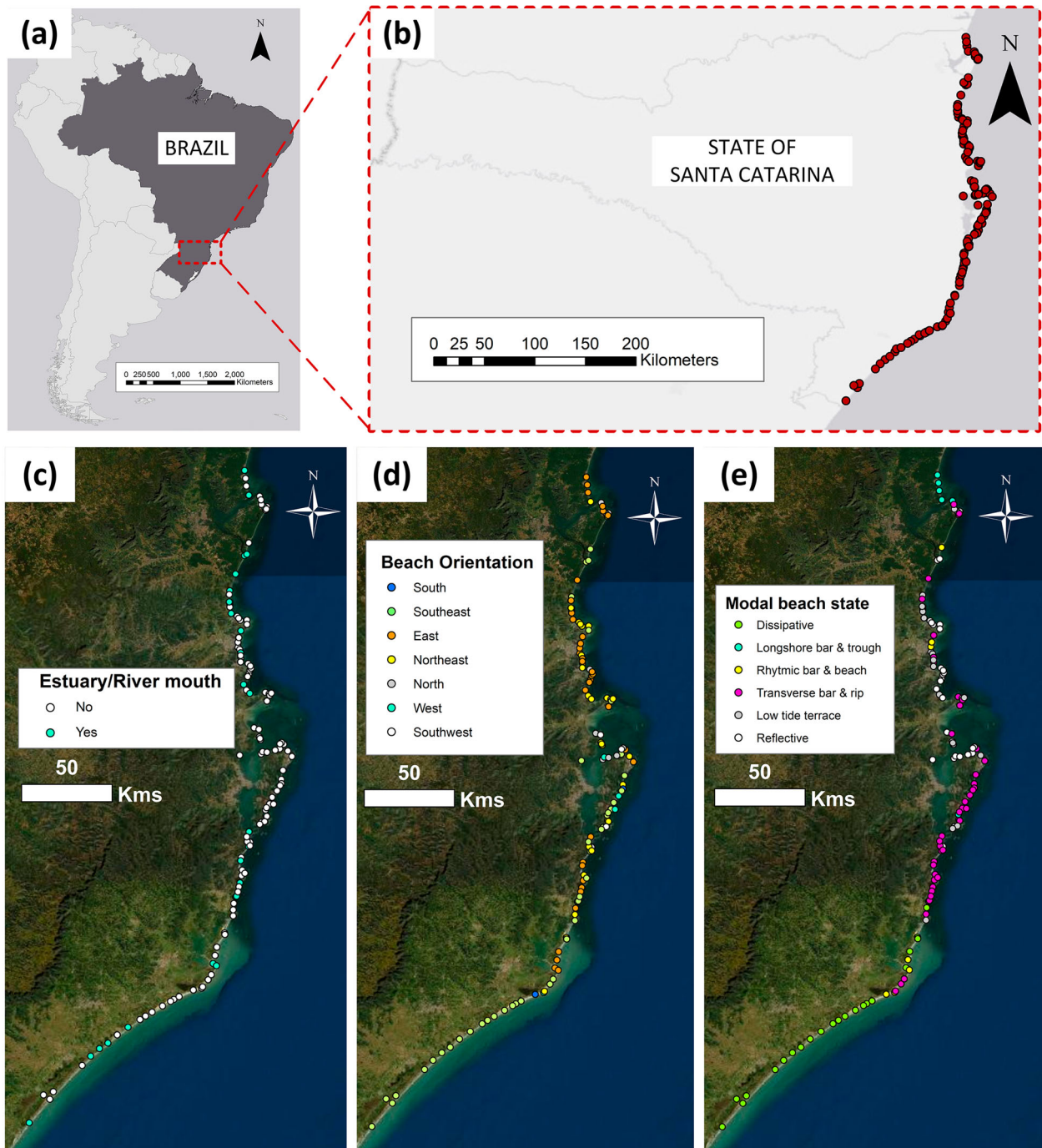


Figure 1. Brazilian coast (a) zooming into the State of Santa Catarina (b) displaying their beach characteristics: (c) presence of an estuary/river mouth, (d) orientation, and (e) annual mean modal state.

The functioning of the DNN is as follows: Each node in the input layer supplies information to every node in the hidden layers through the ‘synapses’. A summation of the contribution of each node in the input layer is performed in each node of the hidden layers by applying an activation function to transform the obtained value. Then, every value of every node in the hidden layers is multiplied by its weight and transmitted to the output node, where another summation is performed by

applying a new activation function to obtain the final output (Wu et al. 2014).

DNNs need to be trained to assign weights accurately and, consequently, minimise errors in the output results (Motamarri and Boccelli 2012). This task depends on the training method and the ratio of the training subset and validating subset to the total data. The training subset is used to estimate unknown connection weights between neurons and the validating subset is used to

Table 1. Characteristics of beach flag warnings data catalogue (2016–2019).

Type	Field	Description
Location	City	Name of the closest city
	Beach	Name of the beach
	Longitude	Longitude of the lifeguard post
	Latitude	Latitude of the lifeguard post
Date	Date	Date when the flag was positioned by the lifeguard
Meteocean conditions	Rip currents	Existence of rip currents (yes/no)
Flag	Flag type	Flag considered by the lifeguard in the post

assess the generalisation ability of the trained network (Maier et al. 2010).

3.2. Methodology to determine electronic bathing flags on beaches using deep neural networks

The proposed methodology integrates operational metocean information from CMEMS and NOAA into a real-time framework by training an artificial neural network with beach flag information to obtain electronic bathing flags at beaches.

This method is divided into five steps (see Figure 3): (1) Setting the DNN arquitecture (Section 3.2.1), (2) Selecting the DNN transfer/activation functions (Section 3.2.2), (3) Determining the DNN training method (Section 3.2.3), (4) Defining the final DNN (Section 3.2.4), and (5) Validating the DNN accuracy to obtain electronic bathing flags (Section 3.2.5).

3.2.1. Setting the DNN architecture

Domain expertise will be needed to frame questions, identify inputs, construct suitable model architectures, and interpret results. There is also evidence that domain expertise of physical principles can improve machine learning outcomes (Ganguly et al. 2014; Karpatne et al. 2017). Regarding beach safety management, input variables are selected using expert criteria by taking into account the main forcings acting on them (metocean conditions) and their geomorphological characteristics (beach conditions). To rank and select the most significant variables, correlation analyses between all candidate variables and beach flag records are conducted.

Next, input variables are categorised to improve data assimilation by the network, because each input variable can collect a very wide range of close values. Categorisation has been used previously in other applications (Brouwer 2002; Nishanth and Ravi 2016), improving the results of the artificial neural systems. This

technique increases the number of input data since, if, for example, we have a variable that can be divided into three ranges, the number of input data for that variable will be three, which will take a value of 1 or 0 depending on the range in which the processed value is found. Each one of the input variables will be categorised to equate the total number of input nodes (n_i) that will feed the DNN.

We then set the number of nodes in the hidden layers (n_h) according to the equation (Equation (1)) as proposed by García-Alba et al. (2019). In addition, we propose to analyse up to a maximum of five hidden layers in order to optimise the network's performance.

$$0.5 \cdot n_i < 2 \cdot n_h \leq 2 \cdot n_i + 2 \quad (1)$$

Lastly, since the DNN output is the electronic bathing flag at one station for every beach, the number of nodes in the output layer (n_o) is one.

3.2.2. Selecting the DNN transfer/activation functions

There are different activation functions for the transfer between the input and the selected hidden layers (including between each of them) and output node (n_o). The most widely activation functions are: sigmoid (Neal 1992) (Equation (2)); hard-sigmoid (Courbariaux et al. 2015) (Equation (3)); hyperbolic tangent (Karlik and Vehbi Olgac 2011) (Equation (4)); softmax (Krizhevsky et al. 2017) (Equation (5)); soft-sign (Turian et al. 2009) (Equation (6)); soft-plus (Dugas et al. 2001) (Equation (7)); Rectified Linear Unit (ReLU) (Zeiler et al. 2013) (Equation (8)); Exponential Linear Unit (ELU) (Clevert et al. 2015) (Equation (9)); and Scaled Exponential Linear Unit (SELU) (Klambauer et al. 2017) (Equation (10)).

$$f(x) = \frac{1}{1 + e^{-x}} \quad (2)$$

$$g(x) = \max\left(0, \min\left(1, \frac{x+1}{2}\right)\right) \quad (3)$$

$$h(x) = \frac{e^x - e^{-x}}{e^x + e^{-x}} \quad (4)$$

$$i(x_i) = \frac{e^{x_i}}{\sum_j e^{x_j}} \quad (5)$$

$$j(x) = \frac{x}{|x| + 1} \quad (6)$$

Table 2. Reanalysis and Forecast metocean data uses in the SOSeas Web Service.

Data type	Forcing	Provider	Product	Variables
Reanalysis	Waves	CMEMS	GLOBAL_REANALYSIS_WAV_001_032	Significant total weight Mean wave period Direction of waves Magnitude of wind velocity Direction of winds Water level variation
	Wind	C3S	ERA 5	Magnitude of wind velocity Direction of winds
	Water level	http://volkov.oce.orst.edu/tides/	TPXO	Water level variation
	Currents	CMEMS	GLOBAL_REANALYSIS_PHY_001_030	Magnitude of marine currents
	Waves	CMEMS	GLOBAL_ANALYSIS_FORECAST_WAV_001_027	Significant total weight Mean wave period Direction of waves Magnitude of wind velocity Direction of winds Water level variation
	Wind	NOAA	Global Forecast System (GFS)	Water level variation Magnitude of marine currents
Forecast	Water level	CMEMS	GLOBAL_ANALYSIS_FORECAST_PHY_001_024	Magnitude of wind velocity Direction of winds
	Currents	CMEMS	GLOBAL_ANALYSIS_FORECAST_PHY_001_024	Water level variation Magnitude of marine currents

where $|x|$ is the absolute value of the input.

$$k(x) = \log(1 + e^x) \quad (7)$$

$$l(x) = \max(0, x) = \begin{cases} x & \text{if } x \geq 0 \\ 0 & \text{if } x < 0 \end{cases} \quad (8)$$

$$m(x) = \begin{cases} x & \text{if } x > 0 \\ \alpha e^x - 1 & \text{if } x \leq 0 \end{cases} \quad (9)$$

where α is the hyperparameter that controls the saturation point for negative net inputs which is usually set to 1.0 (Clevert et al. 2015).

$$n(x) = \lambda \begin{cases} x & \text{if } x > 0 \\ \alpha e^x - \alpha & \text{if } x \leq 0 \end{cases} \quad (10)$$

where λ is the scale factor. The approximate values of the parameters of the SELU function were set to 1.6733 and 1.0507 for α and λ , respectively.

3.2.3. Determining the DNN training method

Several methods are used for training DNNs, with the Adam (Kingma and Ba 2014), Adadelta (Zeiler et al. 2013), Adagrad (McMahan and Streeter 2010), Adamax (Kingma and Ba 2014), Ftrl (McMahan 2014), Nadam (Dozat 2016), RMSprop (Tieleman and Hinton 2012), SGD (Robbins and Monroe 1951) being the most common.

The initial weights are generated randomly to obtain values close to zero. Training and validating are conducted by using a percentage of the total data. This ratio is adjusted by trial and error (Wu et al. 2014).

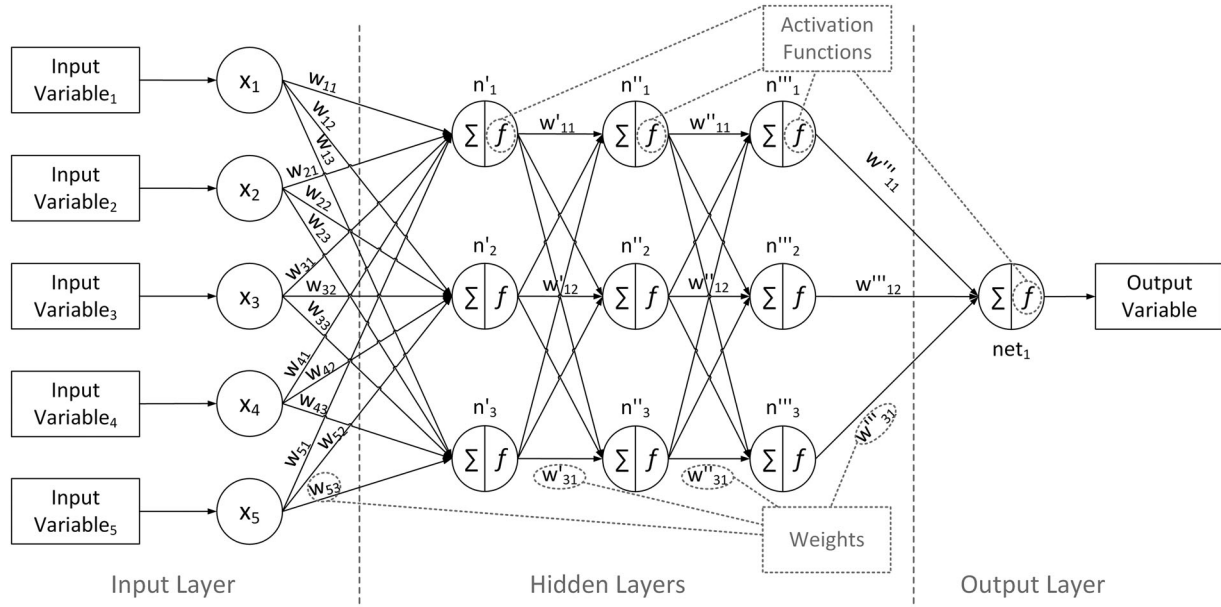


Figure 2. Schematic view of a deep neural network with five nodes in the input layer, three nodes in the three hidden layers and one node in the output layer. Synapses are oriented from left to right.

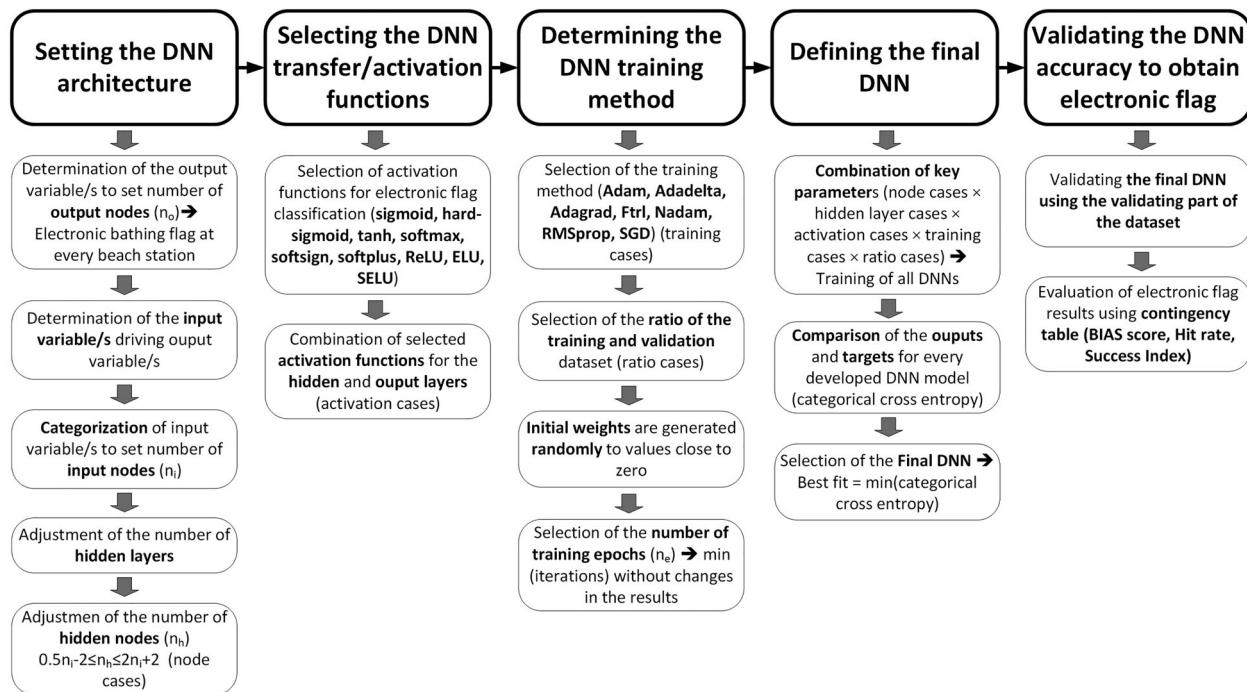


Figure 3. Schematic view of the proposed methodology to develop deep neural networks to obtain electronic bathing flags.

Lastly, the number of training epochs (n_e), learning rate and batch size is decided based on trials by observing the conditions under which DNN training results are independent of the number of iterations (Tufail et al. 2008). The batch size is the number of samples processed before the model is updated and the n_e is the number of complete passes through the training dataset.

3.2.4. Defining the final DNN

The whole group of selected key parameters are combined to develop several DNN models (n_i , n_h , n_o , n_e , training methods, and the ratio of dataset used for training and validating). Next, these models are trained, and the DNN model displaying the lowest error metric between outputs and targets (final DNN) is chosen (Zou et al. 2007). As error metrics, accuracy, bias, hit rate and success index (see Table 3) for the training and validating of the network are used.

In order to assign weights accurately and, consequently, minimise errors in the output results, a loss minimisation function, named the categorical cross-entropy, is used (Equation (11)). It should be noted that this training technique is considered state-of-art performance for DNNs (Goodfellow et al. 2016).

$$\text{Categorical - crossentropy}(p, q) = - \sum_i p_i \cdot \log q_i \quad (11)$$

where q_i is the probability distribution of the predicted data and p_i is the probability distribution of the target data. This function returns the cross-entropy between the approximate (predicted) distribution and the true distribution. It should be noted that the cross-entropy between two probability distributions measures the average number of bits needed to identify an event from a set of possibilities.

3.2.5. DNN performance to classify electronic bathing flags

A contingency table (Table 3) and its error metrics (Table 4) are employed to assess the performance of the final DNN in predicting the electronic bathing flag (Manzato 2007; Bennett et al. 2013; Bedri et al. 2016). Contingency tables establish the number of occurrences where a predictive tool generates correct predictions (see Table 3): (1) hits; (2) the number of alarms missed by the model (misses); and (3) the number of false alarms. Table 5 lists the error metrics of the contingency table used in the current study.

3.3. Setup of deep neural networks for electronic bathing flags in Santa Catarina's beaches

First, n_o was the electronic bathing flag at every station on each beach. The second step was the selection of n_i , based on the correlation analyses between metocean variables and beach flag records, using non-linear

Table 3. Contingency table to assess the performance for the prediction of electronic bathing flags.

		Observed Flag			
		Green	Yellow	Red	
Predicted Flag	Green	Hits	Misses	Misses	Predicted Green
	Yellow	False alarms	Hits	Misses	Predicted Yellow
	Red	False alarms	False alarms	Hits	Predicted Red
		Observed Green	Observed Yellow	Observed Red	

(Spearman) and linear (Pearson) analysis (**Table 5**). Spearman values were always higher than Pearson values for all the variables. This nonlinearity between the metocean conditions and the beach flag records suggests DNNs as a suitable mechanism to predict the dynamic risk of drowning on beaches, based on electronic bathing flags.

Besides the metocean variables collected in **Table 5**, beach orientation and the beach modal state were also considered as input variables because both variables condition breaking wave shape, rip currents, and long-shore currents (Castelle et al. 2016). These three ocean processes are the most potentially harmful to bathers and responsible for about 82% of accidents.

Regarding beach orientation (see **Figure 1(d)**), we transformed this beach characteristic into the incidence angle, i.e. angle between wave direction and beach orientation, as it takes into account temporal variability, providing better results for predicting electronic bathing flags.

Regarding the beach modal state (see **Figure 1(f)**), SCBs were classified by the grain settling Ω (Equation (12) and **Figure 1(d)**), and the relative tidal range RTR (Equation (13) and **Figure 1(e)**) in the following types (Wright and Short 1984; Masselink and Short 1993): (1) Dissipative, (2) Longshore bar and trough, (3)

Rhythmic bar and beach, (4) Transverse bar and rip, (5) Low tide terrace, and (6) Reflective.

$$\Omega = \frac{H_b}{W_s \cdot T_p} \quad (12)$$

$$RTR = \frac{M}{H_b} \quad (13)$$

where H_b is the significant break wave height, T_p is the peak wave period, W_s is the grain settling velocity, and M is the tidal range. The required data to calculate both parameters for every beach were obtained from the studies of Klein et al. (2016) and Quetzalcóatl et al. (2019).

After these analyses, we selected as input variables for the DNN (see **Table 6**): (1) Significant wave height – H_s ; (2) Mean wave period – T_m ; (3) Wind velocity magnitude – W ; (4) Marine current velocity magnitude – U ; (5) Incidence angle – β ; and (6) Beach modal state. As shown in **Table 6**, the categorisation of the DNN input variables was performed by dividing their magnitude into 5, 3, 3, 4, 3 and 6 categories for H_s , T_m , W , U , β , and the beach modal state, respectively.

The final DNN (see **Figure 4**) was obtained using an input layer of categorised variables with a n_i of 6, 3 hidden layers with a n_h of 48, 24 and 24, respectively, and one

Table 4. Error metrics of the contingency table to assess the performance for the prediction of electronic bathing flags (Source: Manzato 2007; Bennett et al. 2013; Bedri et al. 2016).

Metric	Formula	Range	Ideal value	Notes
Accuracy (fraction correct)	$\frac{\text{Hits} + \text{Correct negatives}}{\text{Total}}$	0–1	1	It is influenced by the most common category, usually ‘no event’
Bias score (frequency bias)	$\frac{\text{Hits} + \text{False alarms}}{\text{Hits} + \text{Misses}}$	0– ∞	1	Indicates if the model tends to under- (<1) or over-(>1) estimate
Hit rate (probability of detection)	$\frac{\text{Hits}}{\text{Hits} + \text{Misses}}$	0–1	1	Sensitive to hits but ignore false alarms. Good for rare events
Success index	$\frac{1}{2} \cdot \left(\frac{\text{Hits}}{\text{Hits} + \text{Misses}} + \frac{\text{Hits}}{\text{Hits} + \text{Misses} + \text{False alarms}} \right)$	0–1	1	Equally weighs the ability of the model to correctly detect occurrences and non-occurrences of events

Table 5. Non-linear and linear correlations between the metocean variables and the beach flags collected by SOBRASA lifeguards.

Variables	Correlation				
	Spearman (non-linear)		Pearson (linear)		
	p	$p (<0.0001)$	p	$p (<0.0001)$	
Significant wave height – H_s	0.44	100%	0.41	100%	
Mean wave period – T_m	0.28	100%	0.20	100%	
Wind velocity – W	0.13	100%	0.11	100%	
Marine currents velocity – U	0.08	100%	-0.07	100%	

output layer with a n_o of 1 that created the electronic bathing flag. The transformation of the input variables into the variables of the first hidden layer, as well as between the variables of the hidden layers between them was carried out using the ReLU activation function. This function enables transferring the necessary information from the interactions and non-linearity of the input variables to the deeper layers of the network. The transfer of the last hidden layer to the output node was carried out by a soft-max activation function. This function transforms the information from the nodes of the last hidden layer into probabilities, providing an electronic bathing flag that can take values of green, yellow or red colour. During the training, DNN was optimised using the Adam method. Network optimisation required a n_e of 1000 and a batch-size of 64 to reach a stable situation. For every epoch, a learning rate of 0.001 was used.

Table 6. Categorisation of the DNN input variables in SCB: Significant wave height – H_s ; Mean wave period – T_m ; Wind velocity magnitude – W ; Marine current velocity magnitude – U ; Incidence angle – β ; and Beach modal state.

Conditions	Input Variable (units)	Magnitude	Category
Metocean	Significant wave height – H_s (m)	$H_s \leq 0.5$	Very low
		$0.5 < H_s \leq 1$	Low
		$1 < H_s \leq 1.5$	Moderate
		$1.5 < H_s \leq 2$	High
		$H_s > 2$	Very high
	Mean wave period – T_m (s)	$T_m \leq 7.5$	Low
		$7.5 < T_m \leq 10.6$	Moderate
		$T_m > 10.6$	High
	Wind velocity magnitude – W (m/s)	$W \leq 4.5$	Low
		$4.5 < W \leq 19$	Moderate
Beach	Marine current velocity magnitude – U (m/s)	$W > 9$	High
		$U \leq 0.1$	Low
		$0.1 < U \leq 0.3$	Moderate
		$0.3 < U \leq 0.6$	High
		$U > 0.6$	Very high
	Incidence angle – β (°)	$\beta \leq -45$	Direct
		$45 < \beta \leq 90$	Oblique
		$\beta > 90$	Other
		$f(\Omega, RTR)$	Dissipative
		$f(\Omega, RTR)$	Longshore bar & trough
	Beach modal state	$f(\Omega, RTR)$	Rhythmic bar & beach
		$f(\Omega, RTR)$	Transverse bar & rip
		$f(\Omega, RTR)$	Low tide terrace
		$f(\Omega, RTR)$	Reflective

DNN training and validating were conducted by 90% (71,357 input/output pairs) and 10% (7950 input/output pairs) of the historical flag and input variable data, respectively. The performance of the final DNN was an accuracy of 0.74 and 0.75, a Bias score of 1.03 and 1.03; a hit rate of 0.86 and 0.87; and a success index of 0.80 and 0.81 for the training set and validating set, respectively.

3.4. Implementation of the SOSeas Service: Real time and forecasting of drowning risk.

Operational Systems require having robust and reliable infrastructures to provide services 24 h a day (24/7). A client-server architecture has been adopted to design and implement the SOSeas Service. The SOSeas System architecture (see [Figure 5](#)) is based on a virtualised infrastructure with three main components: (1) numerical analysis and processing components (orange); (2) metocean data management (blue); and (3) web applications (purple).

The metocean data management is operationally undertaken through the collection, standardisation, and storage of metocean data (see [Table 2](#)) in a Data Cube catalogue of NetCDF files. The standardised metocean data can be accessed via interoperability protocols deployed by the middleware THREDDs. As a result, the System provides two ways of communication: machine to machine (M2M) and user-machine interaction.

To provide M2M communication via interoperability protocols, enabling other software to access the system, three Web API Services (Application Programming Interfaces) have been designed: the DataHub API, the SOSeas API, and the Process API. The API acts as an abstraction layer, with a set of rules and specifications, allowing it to be easily used by other software. The DataHub API (<https://datahub.ihcantabria.com/swagger/index.html>) points to any software to access the operational metocean data that is updated constantly. The SOSeas API (<https://apisoseas.ihcantabria.com/swagger/index.html>) provides access to all the lifeguard information, such as events or warnings that could take place on the beach. The Process API (<https://apiprocess.ihcantabria.com/>) provides access to drowning risk assessment on the fly based on the electronic bathing flags calculated by the final DNN.

According to the kind of service provided by the SOSeas Service, the entire system must be monitored 24/7 to ensure the recovery time objective. Therefore, a parallel sub-system monitors all its components (hardware, communication, metocean data, software, etc.) to detect any possible problem or malfunction and expeditiously take the required actions (see the Monitor Server in [Figure 5](#)).

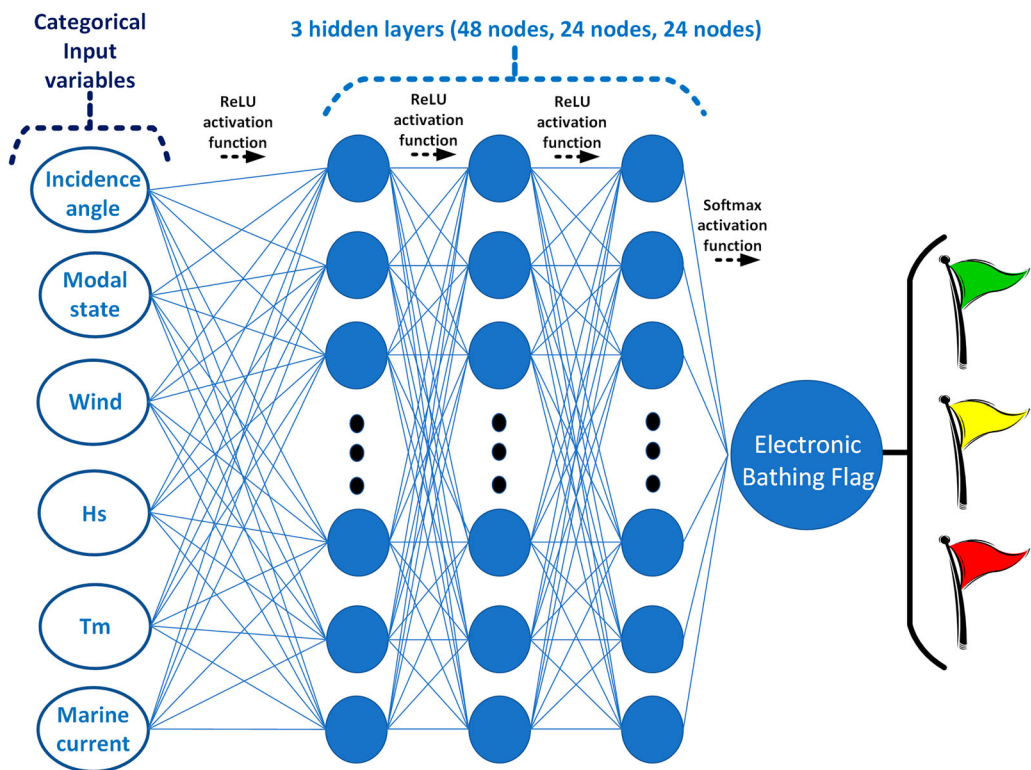


Figure 4. Scheme of the DNN architecture to obtain electronic bathing flag.

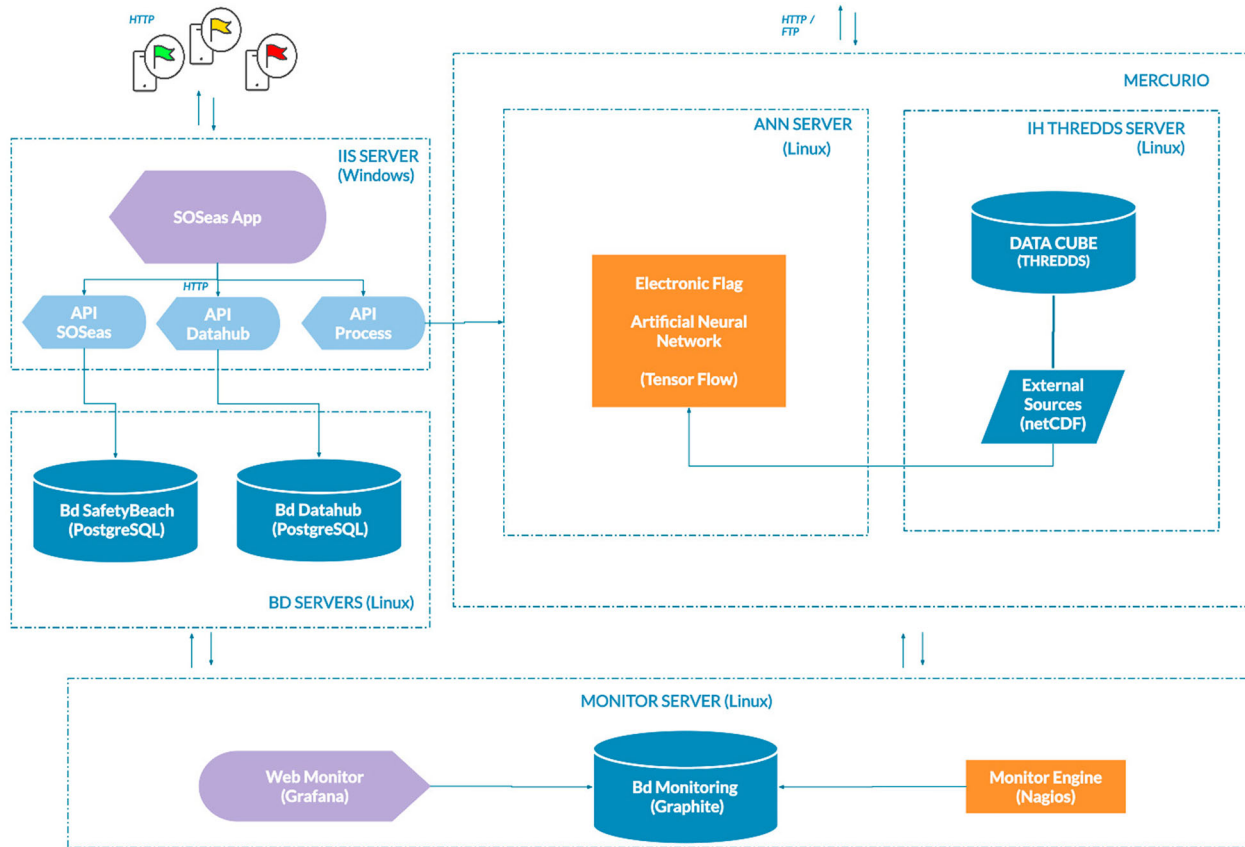


Figure 5. Main components of the SOSeas System.

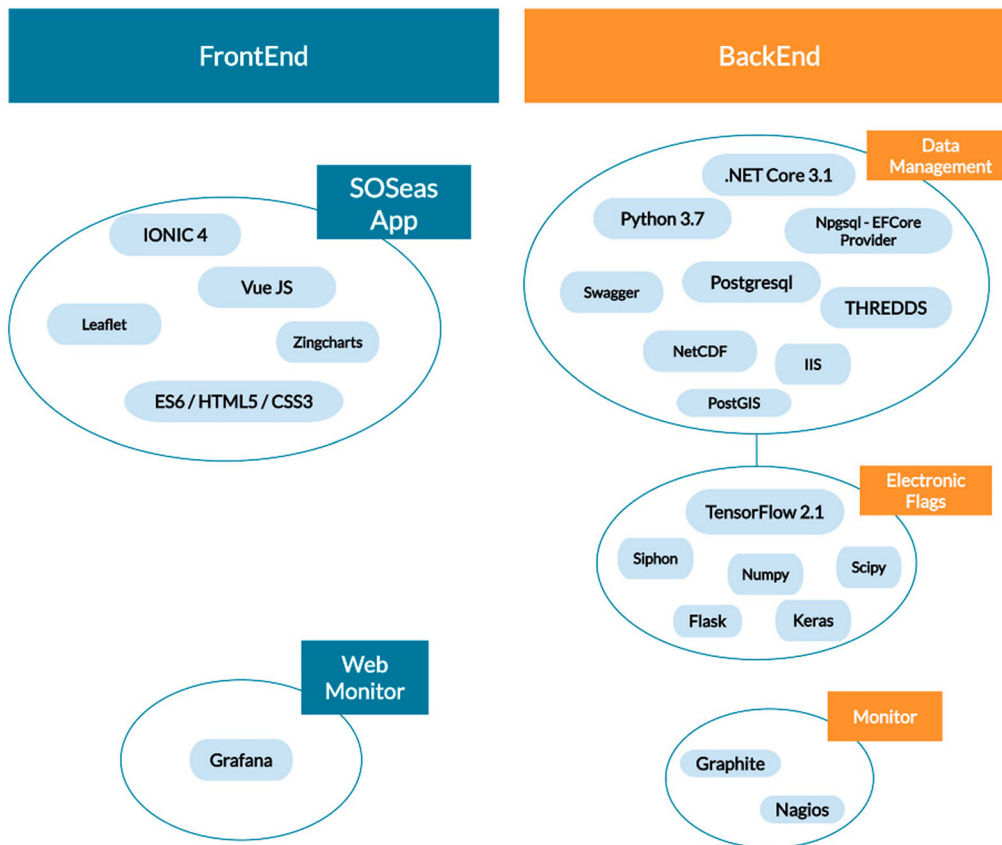


Figure 6. Main software technologies of the SOSeas Service.

The infrastructure required to run the SOSeas Service was composed of two main sections (see Figure 6): Backend (orange) and Frontend (blue), working in a coordinated manner to provide the operational drowning risk. The Frontend includes a friendly user interface available on any web browser and almost any mobile device. Through the App, the user can access all information provided by the system Web APIs, including actual and future beach conditions, in an easy way with attractive and intuitive panels and tables. The Backend gathers and manages the metocean data, performs the analytical and numerical modelling, and provides interoperability protocols. The technologies implemented for the development and maintenance of the Frontend and the Backend of the SOSeas Service are shown in Figure 6.

On the one hand, the Frontend was built by means of the VueJS JavaScript framework. It also used open source libraries for different purposes such as Web Mapping (Leaflet), and graphic visualisation (Zingcharts). A strong point in the app's development is the use of IONIC technology. This technology enables the deployment of the app as a Progressive Web App (PWA), offering a real mobile app feeling in almost any device through any web browser. In addition, IONIC offers the possibility of converting our PWA

into a native IOS and/or Android App. Two types of users, beach users and lifeguards, could interact with the system through the resulting App, which can be downloaded through the SOSeas project Web site (<https://soseas.ihcantabria.com/>).

On the other hand, the Backend was built by means of several technologies for data management: Python (NumPy, SciPy, Keras); .Net (Web APIs, Swagger); relational database management system (PostgreSQL, PostGIS); and THREDDs. Moreover, the Backend used TensorFlow and Keras libraries for the DNN computations. A synthetic description of the different technologies used in the SOSeas Service are collected and displayed in Table S.1 (see Appendix A. Supplementary materials).

In addition to the real time and forecasting of drowning risk, the SOSeas service provides functionalities to store information collected by lifeguards. The app provides a section for the privileged use of lifeguards where they can include events and warnings. The events section collects information about what, when, where and to who, whereas the warning section collects information about preventive actions and warnings. All the information collected could be used to improve the reliability of the ANN.

4. Results

4.1. Electronic bathing flag in Santa Catarina's beaches

Firstly, we determined the annual mean modal state of the 139 coastal beaches studied at SCB (see Figure 1 (e)). The percentage of each modal state at SCB is: (1) Dissipative = 17.05%, (2) Longshore bar and trough = 4.66%, (3) Rhythmic bar and beach = 5.43%, (4) Transverse bar and rip = 34.1%, (5) Low tide terrace = 18.6%, and (6) Reflective = 20.16%. Beaches with a tendency to generate a reflection of the incident energy are more abundant in the study area. Following a south to north direction, SCBs are classified as different transition types between dissipative and reflective beaches. The southern SCBs are mostly catalogued as dissipative while, for the northern SCBs, as reflective. SCBs vary considerably in beach-type and state, though they are dominated in terms of beach length by the higher energy dissipative (31%) and rip-dominated intermediate beaches (46.5%). While the less energetic and least hazardous reflective beaches are the most common and make up only 20% of the beaches by length.

Secondly, Table 7 displays the computed error metrics to assess the performance of the predictive tool in calculating electronic bathing flags at SCB, considering the 100% of the available data (79,487 input/output pairs). Regardless of the used metric in Table 7, the predictive tool presented the following overall (entire SCB) pattern of performance: an accuracy of 0.75; a Bias score of 1.03; a hit rate of 0.87; and a success index of 0.81. Global Bias score shows the DNN trends slightly to overestimate the flag level (yellow flag instead of green flag or red flag instead of yellow flag), a fact on the safe side. Overall, these metrics indicated that the DNN model satisfactorily predicted the electronic bathing flag at SCB.

According to the beach modal state, the success index was ranged between 0.75 and 0.98. Beaches classified as longshore bar and trough due to their modal state obtained the highest success index. On the contrary, beaches

Table 7. Computed metrics to assess the performance of the predictive tool in calculating electronic bathing flags at Santa Catarina's beaches.

Beach modal state of SCB	Data	Accuracy	Bias	Hit rate	Success Index
Dissipative	13,553 (17.05%)	0.76	1.10	0.91	0.84
Longshore bar & trough	3703 (4.66%)	0.98	0.99	0.98	0.98
Rhythmic bar & beach	4316 (5.43%)	0.72	0.96	0.81	0.77
Transverse bar & rip	27,105 (34.10%)	0.71	0.90	0.79	0.75
Low tide terrace	14,785 (18.60%)	0.74	1.12	0.90	0.82
Reflective	16,025 (20.16%)	0.68	1.13	0.86	0.76
Global (All SCB)	79,487 (100%)	0.75	1.03	0.87	0.81

classified as the transverse bar and rip obtained the lowest success index. Accuracy was between 0.68 (reflective) and 0.98 (longshore bar and trough) while, for hit rate, between 0.86 (reflective) and 0.98 (longshore bar and trough).

Lastly, Figure 7(a) shows the success index values obtained for every SCB by the developed tool. Figure 7 also displays three different zooms along the coastal area of Santa Catarina: northern (Figure 7(b)), central (Figure 7(c)), and southern (Figure 7(d)) beaches. As can be seen in Figure 7, the success index values per beach ranges from 0.6 (considered acceptable) to 1 (considered excellent). Beaches displaying a lower success index value (0.6-0.75) were the 31% of SCB. Most of the beaches present a success index value between 0.75 and 0.9, being the 52% of SCB. Beaches presenting the better results, i.e. success index value between 0.9 and 1, were 16% of SCB.

4.2. SOSeas Web App

The resulting SOSeas Web App is accessible at the SOSeas project Web site (<https://soseas.ihcantabria.com/>). Figure 8 shows three sections of the SOSeas Web App. Once the beach has been selected, the home section shows the current metocean conditions and the calculated electronic bathing flag (Figure 8(a)). The beach selection section enables end-users to undertake beach selection based on cities, beach names, or closest distance between the beach and the mobile device (Figure 8(b)). The about section provides information about the SOSeas team, funding and the disclaimer of responsibility of the SOSeas Service (Figure 8(c)).

The SOSeas Web App also provides information about the forecasting conditions through the forecasting section. This section is divided into two subsections: metocean and flags. Graphical visualisations of the metocean subsection for winds and waves are shown in Figure 9(a,c), respectively. Flags subsection makes use of dynamic tables (HTML formatted), which can be visualised in Figure 9(b).

There is also a specific lifeguard section (Figure 10) in the SOSeas Web App where they can manage the beach. The event subsection, see Figure 10(a), enables storing and characterising the events with information such as the type of event, description, consequences, information about the victim, displacement required by lifeguards, etc. Figure 10(b) shows the map subsection with all the geolocated beaches and risks. The warning subsection, see Figure 10(c), enables storing 12 possible preventive actions (e.g. changing flag, detect-marking dangerous places, removing dangerous objects, etc.) and 40 possible preventive warnings (e.g. reporting risks such as currents or solar index, bans, infractions, etc.). Lifeguards with privileges could access the events and warnings subsections.

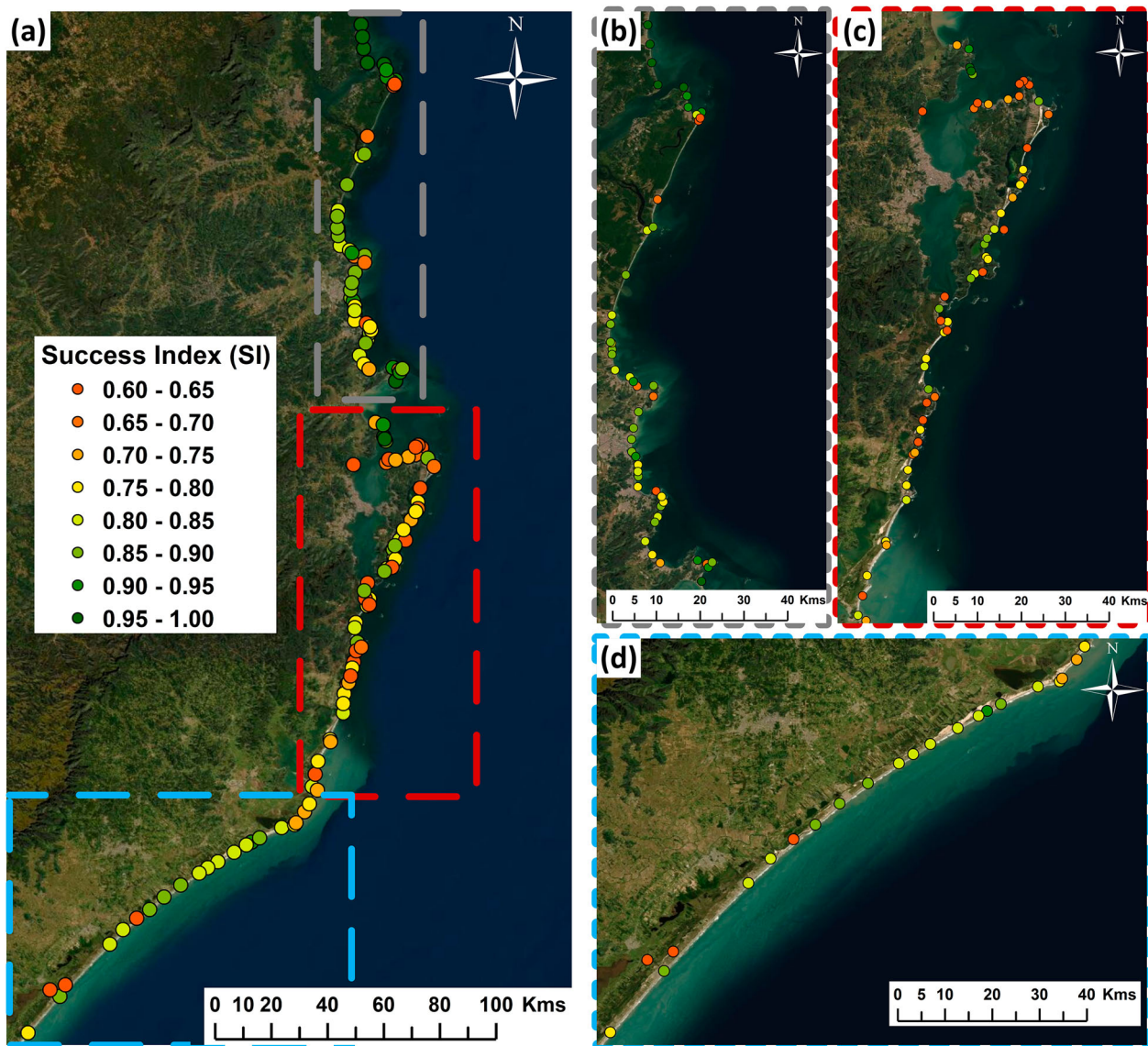


Figure 7. Success index values were obtained with the predictive tool in calculating electronic bathing flags at Santa Catarina's beaches (a), zoomed to the northern (b), central (c), and southern (d) beaches.

Finally, an example of how to use the SOSeas Web App is illustrated in the tutorial Video S.1 (supplementary materials) or the online version: <https://vimeo.com/ihcantabria/SOSeas>.

5. Discussion

5.1. Electronic bathing flag in Santa Catarina's beaches

Three main factors could play a significant role in beach accidents (A. H. Klein et al. 2003): (1) landscape defines the use of coastline and the number of beach users, with embayed beaches the most popular; (2) rip currents are the main natural hazards for bathers (responsible for ~82% of accidents); and (3) the number of people on the

beach contributes. In this sense, we found some issues on the beaches classified as transverse bar and rip. This type of beach produces the highest rip currents; however, they are difficult to predict from the DNN because the transient changes in bathymetry (local effects) are not accounted by the global providers (Meshgrid size = 1/12 degree, approx. 8 km).

According to Wright and Short (1984), reflective beaches present a more violent wave breaking with less wave energy. This is why a reflective beach needs less wave action to become dangerous. This fact is strongly dependent on bathymetry and hinders the classification of the electronic bathing flag because our modal state classification is based on annual mean conditions and does not take into account events of short temporal duration such as storms. These events could temporally modify the beach modal state

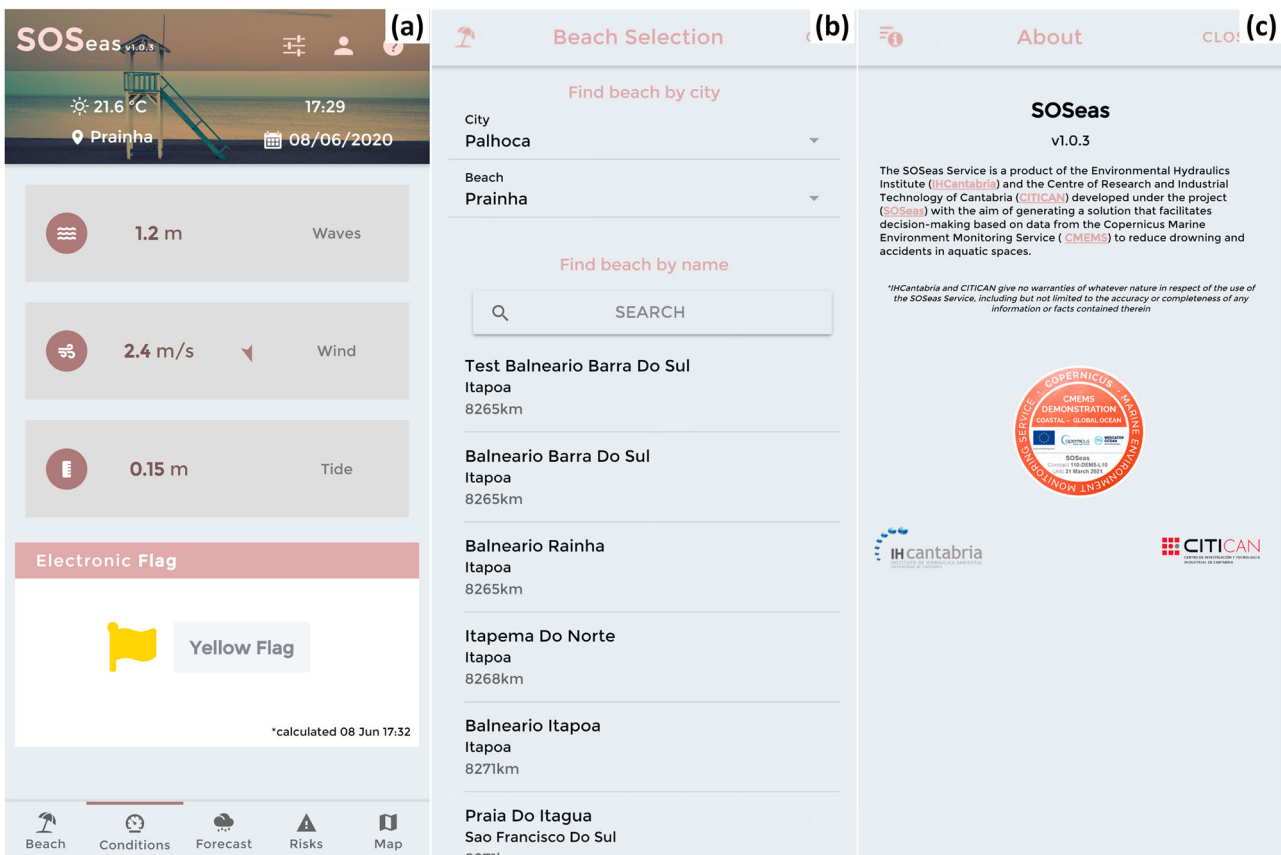


Figure 8. Main tabs of the SOSeas Web App: (a) Web homepage, (b) Beach selection web page, and (c) About SOSeas web page.

and, consequently, the typical action of the metocean forcings in the problem site (Masselink and Short 1993). For this reason, the lowest accuracy of the DNN was obtained for reflective beaches. On the contrary, the best results were obtained from dissipative beaches with bars (longshore and bar) because they show a more stable temporal behaviour and are, thus, better identifiable by the DNN training (Masselink and Short 1993).

It should also be noted that beach modal states considered as the extremes of the modal classification (Wright and Short 1984), i.e. reflective and dissipative, show a Bias score greater than 1. This value indicates the DNN could overestimate the flag warning level. Nevertheless, this fact does not penalise the beach safety status. This phenomenon could be driven by low-occurrence events that modify the metocean patterns at local scales. However, they are not distinguished by the resolution of the global data providers.

In the case of beaches with intermediate modal states, such as rhythmic bar and beach or transverse bar and rip, their mixed behaviour causes the effect of metocean forcing on beach hazardousness more difficult to analyse. This fact could lead to underestimating the electronic bathing flag in these beach typologies.

In this work, we categorised the DNN input variables in SCB based on correlation analyses and expert criteria. However, these class labels might not include information about the relative ordering between labels. Recently, the deep learning community adopted ordinal regression frameworks to consider such ordering information by transforming ordinal targets into binary classification subtasks. Thus, ordinal regression describes the task of predicting labels on an ordinal scale. This feature could help in improving the performance of the DNN by highlighting new categories and ranges for all the input variables (Cao et al. 2020).

Following the issues outlined in our methodology, a better prediction of future DNN applications should consider the following: (1) a temporal evolution of beach modal state; (2) a higher resolution of metocean conditions based on regional (Meshgrid size < 1 km) or local (Meshgrid size < 100 m) data providers; and (3) a new categorisation based on ordinal regression.

5.2. SOSeas Web App

To transfer the dynamic risk of drowning on beaches to society, the SOSeas Web App was designed as an operational system that provides decision support in relation

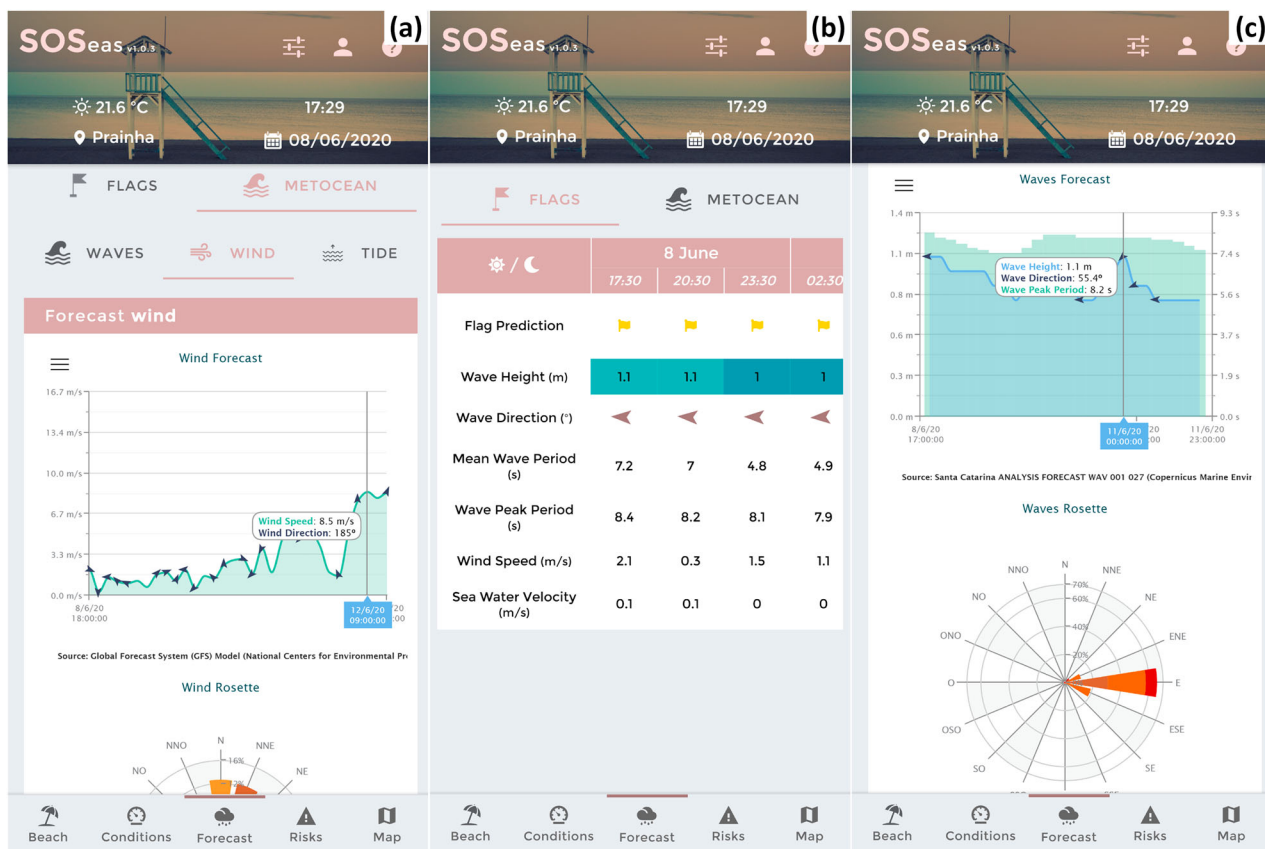


Figure 9. Forecasting section of the SOSeas Web App: (a) Wind conditions, (b) Electronic bathing flags, and (c) Wave conditions.

with metocean phenomena. Decision Support Systems (DSS), and more specifically Environmental Decision Support Systems (EDSS), have adopted Web Technologies aimed at the management of Digital Geographic Information, also called Web Geotechnologies, as a means for the design and construction of capable solutions of representing environmental phenomena (Bhargava et al. 2007; Matthies et al. 2007). Nowadays, the good health of mature open source initiatives (Brovelli et al. 2017) and the scalability of computing environments (Ramamurthy 2016; Raoult and Correa 2016) provide an excellent breeding ground for the design and development of EDSS.

However, the small use of EDSS after their implementations is remarkable (Uran and Janssen 2003; Bolman et al. 2018). Several authors agree that the success of such systems depends on the challenge related to user engagement and emphasise the need for a participatory process that embraces end-users and stakeholders throughout the design and development process (McIntosh et al. 2011). Thus, the implementation of iterative and incremental approaches, commonly used in the IT industry for software development, seems to be a good practice for coastal stakeholder engagement (Heslop et al. 2019;

Fischer et al. 2017). Accordingly, the SOSeas Web App was designed and developed under an iterative and incremental approach by a multidisciplinary team composed by experts in the fields of lifesaving and prevention, hydrodynamics and machine learning, and information technology. Therefore, the authors state an open research line: how beach users can be involved in the design process of coastal EDSS such as the SOSeas Web App?

The degree of support provided by EDSSs is implicit in the knowledge and capabilities of end users (Sánchez-Marré et al. 2008) so the features of the System must be adapted to the type of user (Rizzoli and Young 1997). The SOSeas Web App assumes two levels of knowledge-based information in relation to the type of end-user: (1) beach lifeguards should be familiar with the interpretation of metocean parameters (waves, winds, currents and tides); and (2) beach users should be familiar with standard beach lifeguards communication methods (warning flag system, risk signals, etc.). Therefore, these minimum requirements should be adopted to facilitate the successful implementation of the SOSeas Web App.

Another important aspect is the user experience and how the SOSeas Web App communicates with end-

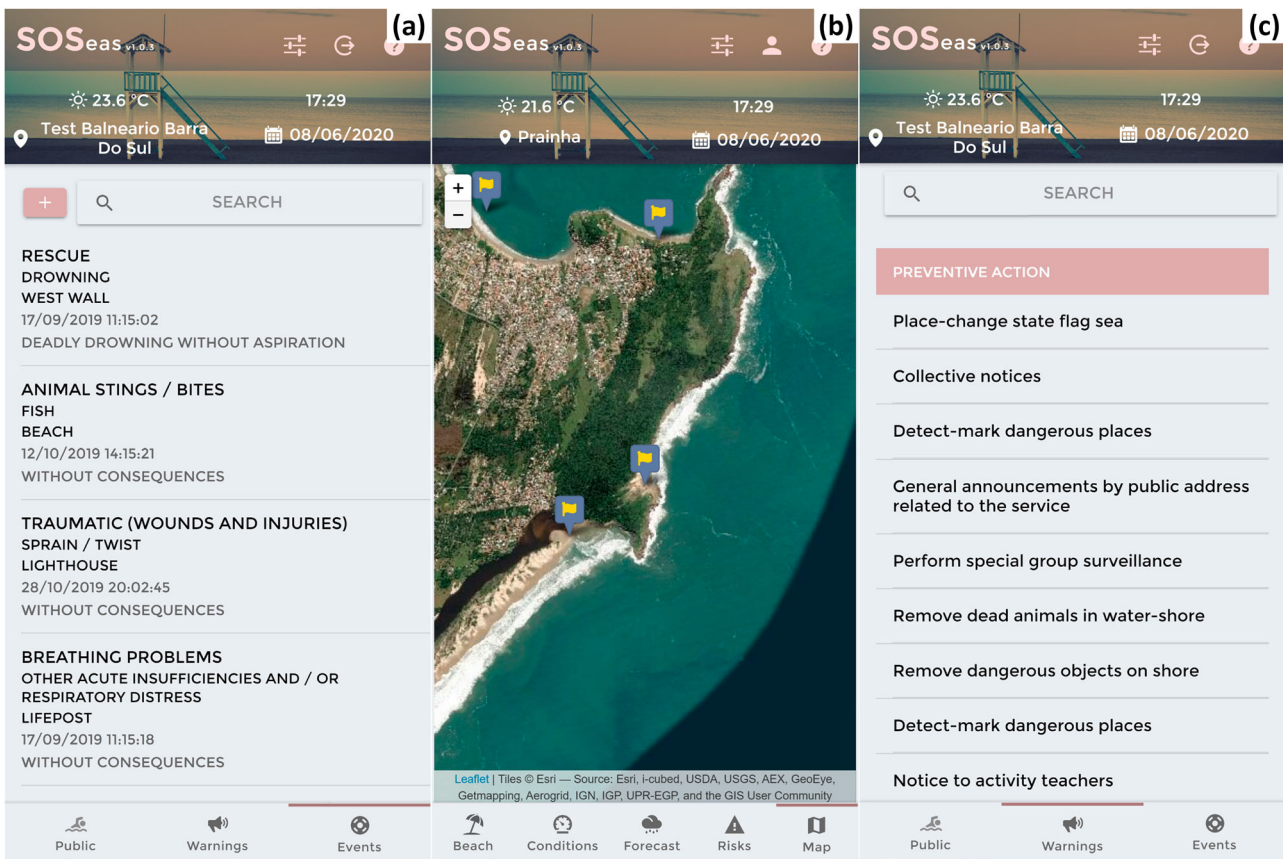


Figure 10. Lifeguard section of the SOSeas Web App: Event subsection (a), Map section (b), and Warning subsection (c).

users. The ubiquity of mobile technologies has opened a wide range of possibilities in the design of EDSS. Two characteristics are essential for the SOSeas Web App: (1) direct communication with end-users enables providing personalised information for each user, and (2) mobile sensors, such as GPS, provide pivotal information in facilitating end-user experiences in a personalised manner.

Lastly, the importance of providing a robust and reliable operational service is key for the successful implementation of the SOSeas Web App. Several factors could affect the SOSeas Web App provision, among them the following dependencies: metocean data providers, communication network between data providers, the SOSeas System and mobile devices, power supply and good performance from the software and hardware hosting the SOSeas Web App.

6. Summary and conclusions

The proposed methodology forecasts electronic bathing flags in beaches for any period by integrating the benefits of a metocean operational system and machine learning into a 24/7 risk assessment service. Thus, the assessment tool has a huge capability of predicting the

effect of metocean forcings on the dynamic risk of drowning on beaches, environments with a high level of non-linear interactions.

First, we performed a crosscutting analysis between metocean conditions, beach characterisations, and flag events catalogue. Secondly, we designed and developed an expert system based on DNN models, to identify the dynamic risk of drowning synchronised to dynamic metocean conditions, followed by obtaining the electronic bathing flags as an indicator of this risk. Thirdly, we applied the proposed methodology to SCB.

The catalogue of events included the information on metocean conditions provided by the CMEMS and the information provided by SOBRASA about flag records in 139 SCB, containing 79,487 records from November 2016 to July 2019. A nonlinear correlation between metocean conditions and beach flags was found, outlining DNN models as suitable for predicting the dynamic risk of drowning on beaches. Additionally, water level variation was also considered another key-variable due to its influence in the wave break form. Thus, the DNN input variables for predicting electronic bathing flags were: (1) Significant wave height – H_s ; (2) Mean wave period – T_m ; (3) Wind velocity magnitude – W ; (4) Marine current

velocity magnitude – U ; (5) Incidence angle – β ; and (6) Beach modal state.

The application of the method to the SCB demonstrated that DNN models are viable surrogates of highly nonlinear process-based models and highly variable forcings to understand the synchronisation between metocean conditions and drowning risks at beaches (chaotic systems). The results showed that the neural networks conveniently reproduced the status flag of beaches and could be easily implemented at any beach worldwide, with low costs of maintenance and high impact in terms of reducing deaths by drowning and rate of accidents in aquatic areas. The SOSeas Web App has created the availability of non-existent tools that enhance safety on beaches.

Through the SOSeas Web App, beach users will be able to have detailed and near real-time information of all risks and their variability along the day. We should mention that lack of knowledge of bathing areas is one of the risk factors that contribute to the increase of drownings and accidents on beaches. Providing information in a predictive manner would therefore help to minimise this risk factor by enabling the selection of the safest spaces at every moment. The SOSeas Web App will also offer the lifeguard services of risk identification and evaluation of the aquatic space they are overseeing. In addition, they will be able to predict future risks for their beaches, enabling them to make decisions that are more efficient on preventive strategies for their environment and helping to reduce accidents and deaths.

Finally, the SOSeas Web App will also provide administrators, such as owners and managers of aquatic spaces, assessment tools for the management and improvement of safety in sandy coastlines. It is important to point that everyone exposed to the inherent risks in these areas, are vulnerable to suffering an accident, by which reducing deaths and accidents grants the administration important savings in healthcare spending. Moreover, improving safety in these areas can also be a source of economic benefit for tourism. Beaches and bathing areas have become a point of interest for national and international tourism, in addition to the increased use made for recreational activities. The creation of safer aquatic spaces generates value as a sign of high-quality tourism.

Acknowledgements

Authors are grateful to the useful and valuable contributions provided by the IHCantabria's staff: Marco Antonio Vega, David Coterillo, David del Prado, Mauricio González, Omar Gutierrez, and Verónica Canovas.

Disclosure statement

No potential conflict of interest was reported by the author(s).

Funding

The European Comission under Copernicus Marine Environment Monitoring Service (CMEMS) User Uptake programme funded this study by means of the contract '110-DEM5-L10'.

References

- Bárcena JF, García-Alba J, García A, Álvarez C. 2016. Analysis of stratification patterns in river-influenced mesotidal and macrotidal estuaries using 3D hydrodynamic modelling and K-means clustering. *Estuarine Coastal Shelf Sci.* 181 (November):1–13. DOI:[10.1016/j.ecss.2016.08.005](https://doi.org/10.1016/j.ecss.2016.08.005).
- Bárcena JF, Gómez AG, García A, Álvarez C, Juanes JA. 2017. Quantifying and mapping the vulnerability of estuaries to point-source pollution using a multi-metric assessment: the Estuarine Vulnerability Index (EVI). *Ecol Indic.* 76 (May):159–169. DOI:[10.1016/j.ecolind.2017.01.015](https://doi.org/10.1016/j.ecolind.2017.01.015).
- Bedri Z, Corkery A, O'Sullivan JJ, Deering LA, Demeter K, Meijer WG, O'Hare G, Masterson B. 2016. Evaluating a microbial water quality prediction model for beach management under the revised eu bathing water directive. *J Environ Manag.* 167:49–58. DOI:[10.1016/j.jenvman.2015.10.046](https://doi.org/10.1016/j.jenvman.2015.10.046).
- Bengio Y, Courville A, Vincent P. 2013. Representation learning: a review and new perspectives. *IEEE Trans Pattern Anal Mach Intell.* 35(8):1798–1828. DOI:[10.1109/TPAMI.2013.50](https://doi.org/10.1109/TPAMI.2013.50).
- Bennett ND, Croke BFW, Guariso G, Guillaume JHA, Hamilton SH, Jakeman AJ, Marsili-Libelli S, et al. 2013. Characterising performance of environmental models. *Environ Model Softw.* 40(February):1–20. DOI:[10.1016/j.envsoft.2012.09.011](https://doi.org/10.1016/j.envsoft.2012.09.011).
- Bhargava HK, Power DJ, Sun D. 2007. Progress in web-based decision support technologies. *Decis Support Syst.* 43 (4):1083–1095. DOI:[10.1016/j.dss.2005.07.002](https://doi.org/10.1016/j.dss.2005.07.002).
- Bolman B, Jak RG, van Hoof L. 2018. Unravelling the myth – the use of decisions support systems in marine management. *Mar Policy.* 87(January):241–249. DOI:[10.1016/j.marpol.2017.10.027](https://doi.org/10.1016/j.marpol.2017.10.027).
- Brouwer RK. 2002. A feed-forward network for input that is both categorical and quantitative. *Neural Netw.* 15 (7):881–890. DOI:[10.1016/S0893-6080\(02\)00090-4](https://doi.org/10.1016/S0893-6080(02)00090-4).
- Brovelli MA, Minghini M, Moreno-Sánchez R, Oliveira R. 2017. Free and Open Source Software for Geospatial Applications (FOSS4G) to support future earth. *Int J Digital Earth.* 10(4):386–404. DOI:[10.1080/17538947.2016.1196505](https://doi.org/10.1080/17538947.2016.1196505).
- Camus P, Losada IJ, Izaguirre C, Espejo A, Menéndez M, Pérez J. 2017. Statistical wave climate projections for coastal impact. *Earth's Future.* 5(9):918–933. DOI:[10.1002/ef2.234](https://doi.org/10.1002/ef2.234).
- Camus P, Mendez FJ, Medina R, Cofiño AS. 2011. Analysis of clustering and selection algorithms for the study of multivariate wave climate. *Coastal Eng.* 58(6):453–462. DOI:[10.1016/j.coastaleng.2011.02.003](https://doi.org/10.1016/j.coastaleng.2011.02.003).

- Cao W, Mirjalili V, Raschka S. 2020. Rank consistent ordinal regression for neural networks with application to age estimation. *Pattern Recognit Lett.* 140(December):325–331. DOI:[10.1016/j.patrec.2020.11.008](https://doi.org/10.1016/j.patrec.2020.11.008).
- Castelle B, Scott T, Brander RW, McCarroll RJ. 2016. Rip current types, circulation and hazard. *Earth Sci Rev.* 163 (December):1–21. DOI:[10.1016/j.earscirev.2016.09.008](https://doi.org/10.1016/j.earscirev.2016.09.008).
- Castelletti A, Galelli S, Ratto M, Soncini-Sessa R, Young PC. 2012. A general framework for dynamic emulation modelling in environmental problems. *Environ Model Softw.* 34 (June):5–18. DOI:[10.1016/j.envsoft.2012.01.002](https://doi.org/10.1016/j.envsoft.2012.01.002).
- Chiri H, Abascal AJ, Castanedo S, José Antonio A. Antolínez, Yonggang Liu, Weisberg RH, Medina R. 2019. Statistical simulation of ocean current patterns using autoregressive logistic regression models: a case study in the Gulf of Mexico. *Ocean Model.* 136(April):1–12. DOI:[10.1016/j.ocemod.2019.02.010](https://doi.org/10.1016/j.ocemod.2019.02.010).
- Chiri H, Abascal AJ, Castanedo S, Medina R. 2019. Mid-long term oil spill forecast based on logistic regression modelling of met-ocean forcings. *Mar Pollut Bull.* 146(September):962–976. DOI:[10.1016/j.marpolbul.2019.07.053](https://doi.org/10.1016/j.marpolbul.2019.07.053).
- Cid A, Camus P, Castanedo S, Méndez FJ, Medina R. 2017. Global reconstructed daily surge levels from the 20th century reanalysis (1871–2010). *Glob Planet Change.* 148:9–21. DOI:[10.1016/j.gloplacha.2016.11.006](https://doi.org/10.1016/j.gloplacha.2016.11.006).
- Cid A, Castanedo S, Abascal AJ, Menéndez M, Medina R. 2014. A high resolution hindcast of the meteorological sea level component for Southern Europe: The GOS dataset. *Clim Dyn.* 43(7–8):2167–2184. DOI:[10.1007/s00382-013-2041-0](https://doi.org/10.1007/s00382-013-2041-0).
- Clevert D-A, Unterthiner T, Hochreiter S. 2015. Fast and accurate deep network learning by Exponential Linear Units (ELUs). 4th International Conference on Learning Representations, ICLR 2016 – Conference Track Proceedings, November. <http://arxiv.org/abs/1511.07289>.
- Courbariaux M, Bengio Y, David J-P. 2015. BinaryConnect: Training Deep Neural Networks with Binary Weights during Propagations. November. <https://github.com/MathieuCourbariaux/BinaryConnect>.
- Dozat T. 2016. Incorporating Nesterov Momentum into Adam. In ICLR Workshop, 2013–16.
- Dugas C, Bengio Y, Belisle F, Nadeau C, Garcia R. 2001. Incorporating second-order functional knowledge for better option pricing. In Neural Information Processing Systems (NIPS), p. 472–478.
- Fischer A, Laak Tt, Bronders J, Desmet N, Christoffels E, van Wezel A, van der Hoek JP. 2017. Decision support for water quality management of contaminants of emerging concern. *J Environ Manag.* 193(May):360–372. DOI:[10.1016/j.jenvman.2017.02.002](https://doi.org/10.1016/j.jenvman.2017.02.002).
- Ganguly AR, Kodra EA, Agrawal A, Banerjee A, Boriah S, Chatterjee S, Chatterjee S, et al. 2014. Toward enhanced understanding and projections of climate extremes using physics-guided data mining techniques. *Nonlinear Process Geophys.* 21(4):777–795. DOI:[10.5194/npg-21-777-2014](https://doi.org/10.5194/npg-21-777-2014).
- García-Alba J, Bárcena JF, Ugarteberu C, García A. 2019. Artificial neural networks as emulators of process-based models to analyse bathing water quality in estuaries. *Water Res.* 150(March):283–295. DOI:[10.1016/j.watres.2018.11.063](https://doi.org/10.1016/j.watres.2018.11.063).
- Goh GB, Hodas NO, Vishnu A. 2017. Deep learning for computational chemistry. *J Comput Chem.* 38(16):1291–1307. DOI:[10.1002/jcc.24764](https://doi.org/10.1002/jcc.24764).
- Gómez AG, Bárcena JF, Juanes JA, Ondiviela B, Sámano ML. 2014. Transport time scales as physical descriptors to characterize heavily modified water bodies near ports in coastal zones. *J Environ Manag.* 136(April):76–84. DOI:[10.1016/j.jenvman.2014.01.042](https://doi.org/10.1016/j.jenvman.2014.01.042).
- Gómez AG, Ondiviela B, Puente A, Juanes JA. 2015. Environmental risk assessment of water quality in harbor areas: a new methodology applied to European ports. *J Environ Manag.* 155(May):77–88. DOI:[10.1016/j.jenvman.2015.01.042](https://doi.org/10.1016/j.jenvman.2015.01.042).
- Goodfellow I, Bengio Y, Courville A. 2016. Deep learning. Cambridge, Massachusetts: MIT Press. <http://www.deeplearningbook.org>.
- Heslop E, Tintoré J, Rotllan P, Álvarez-Berastegui D, Fontera B, Mourre B, Gómez-Pujol L, et al. 2019. SOCIB integrated multi-platform ocean observing and forecasting: from ocean data to sector-focused delivery of products and services. *J Oper Oceanogr.* 12(sup2):S67–S79. DOI:[10.1080/1755876X.2019.1582129](https://doi.org/10.1080/1755876X.2019.1582129).
- Karlik B, Vehbi Olgac A. 2011. Performance analysis of various activation functions in generalized MLP architectures of neural networks. *Int J Artif Intell Expert Syst.* 1(4):111–122. <https://www.cscjournals.org/library/manuscriptinfo.php?mc=IJAE-26>
- Karpatne A, Atluri G, Faghmous JH, Steinbach M, Banerjee A, Ganguly A, Shekhar S, Samatova N, Kumar V. 2017. Theory-guided data science: a new paradigm for scientific discovery from data. *IEEE Trans Knowl Data Eng.* 29 (10):2318–2331. DOI:[10.1109/TKDE.2017.2720168](https://doi.org/10.1109/TKDE.2017.2720168).
- Khalil B, Ouarda TBMJ, St-Hilaire A. 2011. Estimation of water quality characteristics at ungauged sites using artificial neural networks and canonical correlation analysis. *J Hydrol.* 405(3–4):277–287. DOI:[10.1016/j.jhydrol.2011.05.024](https://doi.org/10.1016/j.jhydrol.2011.05.024).
- Kingma DP, Ba J. 2014. Adam: a method for stochastic optimization. 3rd International Conference on Learning Representations, ICLR 2015 – Conference Track Proceedings, December. <https://arxiv.org/abs/1412.6980v9>.
- Klambauer G, Unterthiner T, Mayr A, Hochreiter S. 2017. Self-normalizing neural networks. *Adv Neural Inf Process Syst.* 30:972–981. [http://arxiv.org/abs/1706.02515](https://arxiv.org/abs/1706.02515).
- Klein AH, Santana GG, Diehl FL, de Menezes JT. 2003. Analysis of hazards associated with sea bathing: results of five years work in oceanic beaches of Santa Catarina state, southern Brazil. *J Coast Res.* 35(35):107–116. DOI:[10.2307/40928754](https://doi.org/10.2307/40928754).
- Klein AHdF, Short AD, Bonetti J. 2016. Santa Catarina beach systems. *Coastal Research Library.* 17:465–506. Springer. DOI:[10.1007/978-3-319-30394-9_17](https://doi.org/10.1007/978-3-319-30394-9_17).
- Krizhevsky A, Sutskever I, Hinton GE. 2017. Imagenet classification with deep convolutional neural networks. *Commun ACM.* 60(6):84–90. DOI:[10.1145/3065386](https://doi.org/10.1145/3065386).
- Lunetta P, Smith GS, Penttilä A, Sajantila A. 2004. Unintentional drowning in Finland 1970–2000: a population-based study. *Int J Epidemiol.* 33(5):1053–1063. DOI:[10.1093/ije/dyh194](https://doi.org/10.1093/ije/dyh194).
- Maier HR, Jain A, Dandy GC, Sudheer KP. 2010. Methods used for the development of neural networks for the prediction of water resource variables in river systems: current status and future directions. *Environmental Modelling and Software.* 25(8):891–909. DOI:[10.1016/j.envsoft.2010.02.003](https://doi.org/10.1016/j.envsoft.2010.02.003).

- Manzato A. 2007. Sounding-derived indices for neural network based short-term thunderstorm and rainfall forecasts. *Atmos Res.* 83(2–4):349–365. DOI:[10.1016/j.atmosres.2005.10.021](https://doi.org/10.1016/j.atmosres.2005.10.021).
- Masselink G, Short AD. 1993. The effect of tide range on beach morphodynamics and morphology: a conceptual beach model. *J Coast Res.* 9. <https://journals.flvc.org/jcr/article/view/79047>
- Matthies M, Giupponi C, Ostendorf B. 2007. Environmental decision support systems: current issues, methods and tools. *Environ Model Softw.* 22(2):123–127. DOI:[10.1016/j.envsoft.2005.09.005](https://doi.org/10.1016/j.envsoft.2005.09.005).
- McIntosh BS, Ascough JC, Twery M, Chew J, Elmahdi A, Haase D, Harou JJ, et al. 2011. Environmental decision support systems (EDSS) development – challenges and best practices. *Environ Model Softw.* 26(12):1389–1402. DOI:[10.1016/j.envsoft.2011.09.009](https://doi.org/10.1016/j.envsoft.2011.09.009).
- McMahan HB. 2014. A survey of algorithms and analysis for adaptive online learning. *J Mach Learn Res.* 18(March):1–50. <http://arxiv.org/abs/1403.3465>
- McMahan HB, Streeter M. 2010. Adaptive bound optimization for online convex optimization. *COLT 2010 – The 23rd Conference on Learning Theory*, February, 244–256. <http://arxiv.org/abs/1002.4908>.
- Merwe Rvd, Leen TK, Lu Z, Frolov S, Baptista AM. 2007. Fast neural network surrogates for very high dimensional physics-based models in computational oceanography. *Neural Netw.* 20(4):462–478. DOI:[10.1016/j.neunet.2007.04.023](https://doi.org/10.1016/j.neunet.2007.04.023).
- Motamarri S, Boccelli DL. 2012. Development of a neural-based forecasting tool to classify recreational water quality using fecal indicator organisms. *Water Res.* 46(14):4508–4520. DOI:[10.1016/j.watres.2012.05.023](https://doi.org/10.1016/j.watres.2012.05.023).
- Neal RM. 1992. Connectionist learning of belief networks. *Artif Intell.* 56(1):71–113. DOI:[10.1016/0004-3702\(92\)90065-6](https://doi.org/10.1016/0004-3702(92)90065-6).
- Nishanth KJ, Ravi V. 2016. Probabilistic neural network based categorical data imputation. *Neurocomputing.* 218 (December):17–25. DOI:[10.1016/j.neucom.2016.08.044](https://doi.org/10.1016/j.neucom.2016.08.044).
- Oliveira URd, Barletta RDC, Horn Filho NO. 2014. Distribuição Espacial Das Características Morfodinâmicas Das Praias Arenosas Da Costa Oceânica Da Ilha de Santa Catarina, SC, Brasil. *Pesquisas Em Geociências.* 41(2):89. DOI:[10.22456/1807-9806.78075](https://doi.org/10.22456/1807-9806.78075).
- Peden M, Oyegbite K, Ozanne-Smith J, Hyder AA, Branche C, Rahman AF, Rivara F, Bartolomeos K. 2008. *World report on child injury prevention*. Geneva: World Health Organization.
- Pianca C, Mazzini PLF, Siegle E. 2010. Brazilian offshore wave climate based on NWW3 reanalysis. *Braz J Oceanogr.* 58 (1):53–70. DOI:[10.1590/S1679-87592010000100006](https://doi.org/10.1590/S1679-87592010000100006).
- Polette M, Raucci GD. 2003. Methodological proposal for carrying capacity analysis in sandy beaches: a case study at the central beach of Balneário Camboriú (Santa Catarina, Brazil). *J Coast Res.* 35(35):94–106.
- Quetzalcóatl O, González M, Cánovas V, Medina R, Espejo A, Klein A, Tessler MG, et al. 2019. SMC_e, a coastal modeling system for assessing beach processes and coastal interventions: application to the Brazilian coast. *Environ Model Softw.* 116. doi:[10.1016/J.ENVSOF.2019.03.001](https://doi.org/10.1016/J.ENVSOF.2019.03.001).
- Raghu M, Poole B, Kleinberg J, Ganguli S, Sohl-Dickstein J. 2016. On the expressive power of deep neural networks. *Beitr Entomol.* 3(1):116–162. DOI:[10.1606/05336](https://doi.org/10.1606/05336).
- Ramamurthy M. 2016. Data-driven atmospheric sciences using cloud-based cyberinfrastructure. *Cloud Comput Ocean Atmosph Sci.* 43–58. Elsevier. DOI:[10.1016/B978-0-12-803192-6.00004-9](https://doi.org/10.1016/B978-0-12-803192-6.00004-9).
- Raoult B, Correa R. 2016. Cloud computing for the distribution of numerical weather prediction outputs. *Cloud Comput Ocean Atmosph Sci.* 121–135. Elsevier. DOI:[10.1016/B978-0-12-803192-6.00008-6](https://doi.org/10.1016/B978-0-12-803192-6.00008-6).
- Rizzoli AE, Young WJ. 1997. Delivering environmental decision support systems: software tools and techniques. *Environ Model Softw.* 12(2–3):237–249. DOI:[10.1016/S1364-8152\(97\)00016-9](https://doi.org/10.1016/S1364-8152(97)00016-9).
- Robbins H, Monroe S. 1951. A stochastic approximation method. *Ann Math Stat.* 22(3):400–407. DOI:[10.1214/aoms/1177729586](https://doi.org/10.1214/aoms/1177729586).
- Sánchez-Marrè M, Gibert K, Sojda RS, Steyer JP, Struss P, Rodríguez-Roda I, Comas J, Brilhante V, Roehl EA. 2008. Chapter eight intelligent environmental decision support systems. *Dev Integr Environ Assess.* 3:119–144. Elsevier. DOI:[10.1016/S1574-101X\(08\)00608-X](https://doi.org/10.1016/S1574-101X(08)00608-X).
- Schmidhuber J. 2015. Deep learning in neural networks: an overview. *Neural Netw.* 61:85–117. DOI:[10.1016/j.neunet.2014.09.003](https://doi.org/10.1016/j.neunet.2014.09.003).
- Shen C. 2018. A transdisciplinary review of deep learning research and its relevance for water resources scientists. *Water Resour Res.* 54(11):8558–8593. DOI:[10.1029/2018WR022643](https://doi.org/10.1029/2018WR022643).
- Szpilman D, Bierens JJLM, Handley AJ, Orlowski JP. 2012. Drowning. *N Engl J Med.* 366(22):2102–2110. DOI:[10.1056/NEJMra1013317](https://doi.org/10.1056/NEJMra1013317).
- Tieleman T, Hinton G. 2012. Lecture 6.5-Rmsprop: divide the gradient by a running average of its recent magnitude. COURSERA: Neural Netw Mach Learn. 4:26–30. <https://www.coursera.org/lecture/deep-neural-network/rmsprop-BhJlm>.
- Traon PYL, Reppucci A, Alvarez Fanjul E, Aouf L, Behrens A, Belmonte M, Bentamy A, et al. 2019. From observation to information and users: The Copernicus marine service perspective. *Front Mar Sci.* 6(May):234. DOI:[10.3389/FMARS.2019.00234](https://doi.org/10.3389/FMARS.2019.00234).
- Tufail M, Ormsbee L, Teegavarapu R. 2008. Artificial intelligence-based inductive models for prediction and classification of fecal coliform in surface waters. *J Environ Eng.* 134 (9):789–799. DOI:[10.1061/\(ASCE\)0733-9372\(2008\)134:9\(789\)](https://doi.org/10.1061/(ASCE)0733-9372(2008)134:9(789)).
- Turian J, Bergstra J, Bengio Y. 2009. Quadratic features and deep architectures for chunking. In *Proceedings of Human Language Technologies: The 2009 Annual Conference of the North American Chapter of the Association for Computational Linguistics, Companion Volume: Short Papers on - NAACL '09*, 245. Morristown, NJ, USA: Association for Computational Linguistics. <https://doi.org/10.3115/1620853.1620921>.
- Uran O, Janssen R. 2003. Why are spatial decision support systems not used? Some experiences from the Netherlands. *Comput Environ Urban Syst.* 27(5):511–526. DOI:[10.1016/S0198-9715\(02\)00064-9](https://doi.org/10.1016/S0198-9715(02)00064-9).
- Washington WM, Buja L, Craig A. 2009. The computational future for climate and earth system models: on the path to petaflop and beyond. *Philos Trans R Soc A: Math Phys Eng Sci.* 367(1890):833–846. DOI:[10.1098/rsta.2008.0219](https://doi.org/10.1098/rsta.2008.0219).

- WHO. 2014. Global report on drowning: preventing a leading killer. World Health Organisation. http://www.who.int/violence_injury_prevention/global_report_drowning/en/.
- Wright LD, Short AD. 1984. Morphodynamic variability of surf zones and beaches: a synthesis. Mar Geol. 56(1-4):93–118. DOI:[10.1016/0025-3227\(84\)90008-2](https://doi.org/10.1016/0025-3227(84)90008-2).
- Wu W, Dandy GC, Maier HR. 2014. Protocol for developing ANN models and its application to the assessment of the quality of the ANN model development process in drinking water quality modelling. Environmental Modelling and Software. 54:108–127. DOI:[10.1016/j.envsoft.2013.12.016](https://doi.org/10.1016/j.envsoft.2013.12.016).
- Yosinski J, Clune J, Bengio Y, Lipson H. 2014. How transferable are features in deep neural networks? Adv Neural Inf Process Syst. 4(January):3320–3328. <http://arxiv.org/abs/1411.1792>
- Zeiler MD, Ranzato M, Monga R, Mao M, Yang K, Le QV, Nguyen P, et al. 2013. On Rectified Linear Units for Speech Processing. In 2013 IEEE International Conference on Acoustics, Speech and Signal Processing, 3517–21. IEEE. <https://doi.org/10.1109/ICASSP.2013.6638312>.
- Zeng X, Li Y, He R. 2015. Predictability of the loop current variation and eddy shedding process in the Gulf of Mexico using an artificial neural network approach. J Atmos Ocean Technol. 32(5):1098–1111. DOI:[10.1175/JTECH-D-14-00176.1](https://doi.org/10.1175/JTECH-D-14-00176.1).
- Zou R, Lung W-S, Wu J. 2007. An adaptive neural network embedded genetic algorithm approach for inverse water quality modeling. Water Resour Res. 43(8):1–13. DOI:[10.1029/2006WR005158](https://doi.org/10.1029/2006WR005158).